EUKARYOTIC CELL, Apr. 2005, p. 755–764 Vol. 4, No. 4
1535-9778/05/$08.00+0 doi:10.1128/EC.4.4.755–764.2005

Pairwise Knockdowns of cdc2-Related Kinases (CRKs) in *Trypanosoma brucei* Identified the CRKs for G_1/S and G_2/M Transitions and Demonstrated Distinctive Cytokinetic Regulations between Two Developmental Stages of the Organism

Xiaoming Tu and Ching C. Wang*

Department of Pharmaceutical Chemistry, University of California, San Francisco, California

Received 7 February 2005/Accepted 15 February 2005

Expression of the cdc2-related kinase 3 (CRK3) together with expression of CRK1, -2, -4, or -6, were knocked down in pairs in the procyclic and bloodstream forms of *Trypanosoma brucei*, using the RNA interference technique. Double knockdowns of CRK3 and CRK2, CRK4, or CRK6 exerted significant growth inhibition and enriched the cells in G_2/M phase, whereas a CRK3 plus CRK1 (CRK3 + CRK1) knockdown arrested cells in both G_1/S and G_2/M transitions. Thus, CRK1 and CRK3 are apparently the kinases regulating the G_1/S and G_2/M checkpoint passages, respectively, whereas the other CRKs are probably playing only minor roles in cell cycle regulation. A CRK1 + CRK2 knockdown in the procyclic form was found to cause aberrant posterior cytoskeletal morphogenesis (X. M. Tu and C. C. Wang, Mol. Biol. Cell 16:97–105, 2005). A CRK3 + CRK2 knockdown, however, did not lead to such a change, suggesting that CRK2 depletion can lead to the abnormal morphogenesis only when procyclic-form cells are arrested in the G_1 phase. The G_2/M-arrested procyclic form produces up to 20% stumpy anucleated cells (zoids) in the population, suggesting that cytokinesis and cell division are not blocked by mitotic arrest but are apparently driven to completion by the kinetoplast cycle. In the bloodstream form, however, G_2/M arrest resulted in little zoid formation but, instead, enriched a population of cells each containing multiple kinetoplasts, basal bodies, and flagella and an aggregate of multiple nuclei, indicating failure in entering cytokinesis. The two different cytokinetic regulations between two distinct stage-specific forms of the same organism may provide an interesting and useful model for further understanding the evolution of cytokinetic control among eukaryotes.

African trypanosomes are among the most ancient eukaryotic microorganisms, with an ancestry occasionally reflected in unusual biology. *Trypanosoma brucei* is the causative agent of several diseases in mammals, including nagana in cattle and human sleeping sickness. *T. brucei* has a biphasic life cycle. The bloodstream form in mammals and the procyclic form in the alimentary tract of the tsetse fly are the two dividing forms that establish infections. They differ significantly in many biochemical and metabolic aspects due to their distinctive living environments (29).

A trypanosome cell has four major organelles that are known to play important roles in cell division: the nucleus; a single mitochondrion extending from one to the other cellular end with a mitochondrial DNA complex; the kinetoplast, an extramitochondrial basal body connected to the kinetoplast across the mitochondrial membrane; and a flagellum subtended from the basal body (8). These organelles must be accurately replicated and correctly segregated in a well-coordinated manner to drive cell division, thus suggesting novel mechanisms in trypanosome cell cycle control. Trypanosomes have the usual sequential G_1, S, G_2, and M phases in its cell cycle (36), but it differs from other organisms by the presence of a kinetoplast cell cycle with an S phase (S_K) and a phase of kinetoplast segregation preceding the nuclear S phase (S_N) and mitosis, respectively (21, 36). In the procyclic form of *T. brucei*, early events in the G_1 phase are the maturation of a pro-basal body next to the existing basal body, the outgrowth from it of a daughter flagellum, and the commencement of kinetoplast S phase (24, 36). Segregation of the duplicated basal bodies, kinetoplasts, and flagella occur in early G_2 (22, 23). Mitosis then places one of the resulting daughter nuclei between the two kinetoplasts, ensuring correct partitioning of the organelles, when the cleavage furrow bisects the cell from the anterior to the posterior end in a helical fashion (24).

Far less is known about the cell cycle events in the bloodstream form of *T. brucei*, which has a much shorter cell length than the procyclic form and its kinetoplast is located at the far posterior end of the cell instead of the midregion as in the procyclic form (16). These distinctions may explain why, following mitosis in the bloodstream form, there is no migration of one of the two nuclei to the location between the two segregated kinetoplasts (16). There thus could be differences in the mechanisms of cytokinesis regulation and cell division between the two forms.

There are three mitotic cyclin homologues in *T. brucei*, among which a knockdown of CycB2/CYC6 expression by RNA interference (RNAi) was sufficient for arresting cells of both forms in G_2/M phase (9, 14). In the procyclic form, the arrest generated stumpy anucleated cells (zoids) up to about 15% of the total population, suggesting continued cytokinesis

* Corresponding author. Mailing address: Department of Pharmaceutical Chemistry, UCSF, San Francisco, CA 94143-2280. Phone: (415) 476-1321. Fax: (415) 476-3382. E-mail: ccwang@cgl.ucsf.edu.

and cell division in the absence of mitosis (14). But only cells with one nucleus and multiple kinetoplasts were observed in the arrested bloodstream form, indicating that cytokinesis is blocked when mitosis is inhibited even though the kinetoplast cycle continues to proceed (9).

Five cdc2-related kinases (CRKs), 1, 2, 3, 4, and 6, were identified in the *T. brucei* genome (8, 19). An RNAi knockdown of CRK3 expression reduced the growth of the procyclic form by 91% and the bloodstream form by 69% with an enrichment of cells in the G_2/M phases in both forms (26). The arrested procyclic form contained 20% stumpy zoids in the population, whereas the bloodstream form had an enriched population of cells with one nucleus and two kinetoplasts and a small population containing aggregated multiple nuclei and multiple kinetoplasts. These results confirmed and expanded previous observations resulting from cyclin knockdown. But neither study provided a clear demonstration of the precise point of arrest of the cell cycle events in the bloodstream form.

The RNAi knockdown of CRK3 did not block cell growth completely or achieve total G_2/M arrest in either the procyclic or bloodstream form (26). We thus tried in the present study further RNAi knockdowns of CRK3 paired with another CRK (1, 2, 4, or 6) to test for potential involvement of another CRK in regulating the G_2/M checkpoint passage. We also examined the distribution of nuclei, kinetoplasts, basal bodies, and flagella in the bloodstream-form cells arrested in G_2/M and identified, by DNA staining and immunofluorescence, equal multiplicity of kinetoplasts, basal bodies, and full-length flagella in each cell, suggesting a kinetoplast cycle operating and progressing in mitotically arrested cells but incapable of entering cytokinesis.

MATERIALS AND METHODS

Cell cultures. Procyclic-form *T. brucei* strain 29-13 (34) was cultivated at 26°C in Cunningham's medium supplemented with 10% fetal bovine serum (Atlanta Biological). G418 (15 μg/ml) and hygromycin B (50 μg/ml) were maintained in the culture medium to preserve the T7 RNA polymerase and tetracycline repressor gene constructs within the cells.

Bloodstream-form *T. brucei* strain 90-13 (34) was cultivated at 37°C in HMI9 medium supplemented with 10% fetal bovine serum and 10% serum plus (JRH Biosciences) (11). G418 (2.5 μg/ml) and hygromycin B (5 μg/ml) were also added to the culture medium to stabilize the intracellular plasmids.

RNAi. A partial cDNA fragment (~250 to 550 bp in length) of each of the five *T. brucei* CRK genes (the GenBank accession numbers of the CRK1, CRK2, CRK3, CRK4, and CRK6 genes are X64314, X74598, X74617, AJ413200, and AJ505556, respectively) was amplified by PCR using a pair of gene-specific primers (sequences available upon request) and paired as follows: CRK3 plus CRK1 (CRK3 + CRK1), CRK3 + CRK2, CRK3 + CRK4, and CRK3 + CRK6. Each pair of PCR fragments was ligated together and subcloned into the pZJM vector by replacing the α-tubulin fragment in it (31). The resulting RNAi construct was linearized with NotI and transfected into *T. brucei* for integration into the rRNA gene spacer region in the *T. brucei* chromosome.

Transfection of procyclic-form *T. brucei* with the linearized DNA construct by electroporation was performed essentially according to previously described procedures (26). Electroporation was carried out in a 2-mm cuvette using a Gene Pulser (Bio-Rad) with parameters set at 1.6-kV voltage, 400-Ω resistance, and 25-μF capacitance. The electroporated cells were immediately transferred to SDM-79 medium and incubated at 26°C for 24 h. Transfectants were selected under 2.5 μg/ml phleomycin.

Transfection of bloodstream-form *T. brucei* was performed as previously described (26). Briefly, a sample of 1×10^7 log-phase cells was harvested, washed once with cytomix buffer (19a), and suspended in 0.5 ml of the same buffer containing 100 μg of the linearized pZJM DNA construct described above. Electroporation was carried out in a 4-mm cuvette using the Gene Pulser (Bio-Rad) with parameters set at 1.7-kV voltage, 400-Ω resistance, and 25-μF capacitance. The electroporated cells were transferred immediately to a 24-well plate in HMI 9 medium and incubated at 37°C for 24 h. Transfectants were then selected with the addition of 2.5-μg/ml phleomycin.

Individual transfectants were cloned on a 0.6% agarose plate (2), and the cloned transfectants were each grown in culture medium containing phleomycin. Transcription of the DNA insert was induced by adding 1 μg/ml tetracycline to the culture to switch on the T7 promoter. The double-stranded RNA thus synthesized is expected to lead to specific degradation of its corresponding mRNA in *T. brucei* (1, 13, 17, 25). To evaluate the potential effect from the mRNA degradation on cell proliferation, the cells were counted at different times after RNAi induction using a hemocytometer.

Semiquantitative RT-PCR. Total RNA was extracted from *T. brucei* cells using the TRIzol reagent (Amersham Pharmacia), and DNase I was added to the RNA extract to digest the remaining DNA. Reverse transcription-PCR (RT-PCR) was then performed using the one-step RT-PCR kit (Invitrogen) and a pair of gene-specific primers that differed from the primer pair used in generating the original RNAi construct (sequences available upon request).

FACS analysis. Cell samples for fluorescence-activated cell sorting (FACS) analysis were prepared as described previously (26). Briefly, samples of the transfected *T. brucei* cells (2×10^6 cells) were collected before and during tetracycline induction, centrifuged at 2,500 × *g* and 4°C for 10 min, and washed twice in phosphate-buffered saline (PBS; 137 mM NaCl, 8 mM KCl, 10 mM Na_2HPO_4, 2 mM KH_2PO_4, pH 7.4). The cell pellets were gently suspended in 100 μl of PBS and mixed with 200 μl of 10% ethanol/5% glycerol in PBS. They were then mixed with another 200 μl of 50% ethanol/5% glycerol prior to incubation on ice for 5 min. One milliliter of 70% ethanol/5% glycerol was then added, and the mixture was left at 4°C overnight.

The cells were washed with PBS twice and suspended in PBS. DNase-free RNase (Sigma) and propidium iodide (PI) were added to the suspension to final concentrations of 10 μg/ml and 20 μg/ml, respectively, and incubated for 30 min at room temperature before the FACS analysis. The DNA content of PI-stained cells was analyzed with a FACScan analytical flow cytometer using CELLQuest software (Becton Dickinson). Percentages of cells in each phase of the cell cycle, G_1, S, and G_2/M, were determined with ModFitLT V3.1 software (Becton Dickinson). The same PI-stained cell samples were also examined under an Olympus phase-contrast and fluorescence microscope for tabulating numbers of nuclei and kinetoplasts in individual cells and counting cells with different morphologies from a population of about 200 cells.

Immunofluorescence microscopy. Cells were harvested, washed with PBS three times, and fixed as described previously (27). Alternatively, they were fixed in cold methanol at −20°C for 20 min and then washed three times with PBS. The fixed cells were blocked in the blocking buffer (2% bovine serum albumin and 0.1% Triton X-100 in PBS) for 60 min at room temperature and incubated with a primary antibody for 60 min at room temperature. The following primary antibodies were used: YL1/2 (Chemicon; rat monoclonal antibodies against yeast tyrosinated α-tubulin, 1:400 dilution) and ROD1 (from Keith Gull, Oxford University; mouse monoclonal antibody against the paraflagellar rod protein [PFR], no dilution). Fluorescein isothiocyanate- or Cy3-conjugated secondary goat antibodies (Sigma), including fluorescein isothiocyanate–anti-rat immunoglobulin G (diluted 1:400) and Cy3–anti-mouse immunoglobulin G (diluted 1:300), were then applied, and the cells were incubated for another 60 min at room temperature. Slides were mounted in Vectashield in the presence of 1 μg of 4′,6′-diamidino-2-phenylindole (DAPI) per ml and examined with a fluorescence microscope.

RESULTS

Simultaneous RNA interference with expression of *CRK3* and another *CRK* gene in *T. brucei*. We employed the RNAi technique to knock down expression of *CRK3* and another *CRK* gene (*CRK1*, *CRK2*, *CRK4*, or *CRK6*) from *T. brucei* simultaneously. An ~250- to 500-bp DNA fragment of a unique sequence from the coding region of each gene that has no significant sequence identity with the rest of the genome sequences in the Trypanosome Genome Database was amplified by PCR. Each pair of the PCR fragments (totaling four combinations: *CRK3* + *CRK1, CRK3* + *CRK2, CRK3* + *CRK4*, and *CRK3* + *CRK6*) was ligated together in the indicated order and subcloned into the RNAi vector pZJM (31). The newly generated sequence around the junction of ligation in each

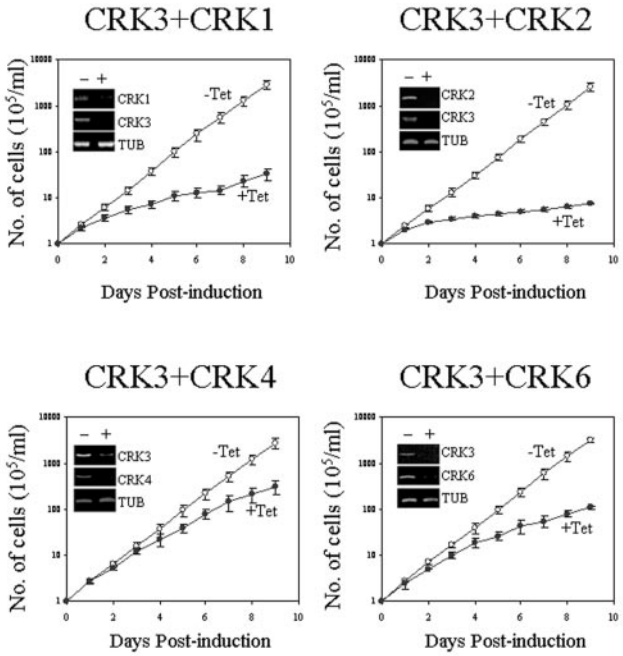

FIG. 1. Effects of double CRK knockdowns on the growth of procyclic-form *T. brucei* cells. Cloned procyclic trypanosome cells harboring the double CRK RNAi plasmid constructs were each incubated in culture medium containing 1.0-μg/ml tetracycline (+Tet) at 26°C. Cell growth was monitored daily, and the cell numbers plotted in a logarithmic scale. The insets show the intracellular mRNA levels in the cells after a 3-day RNAi induction monitored by semiquantitative RT-PCR. Quantitation of α-tubulin mRNA (*TUB*) was included as a sampling control.

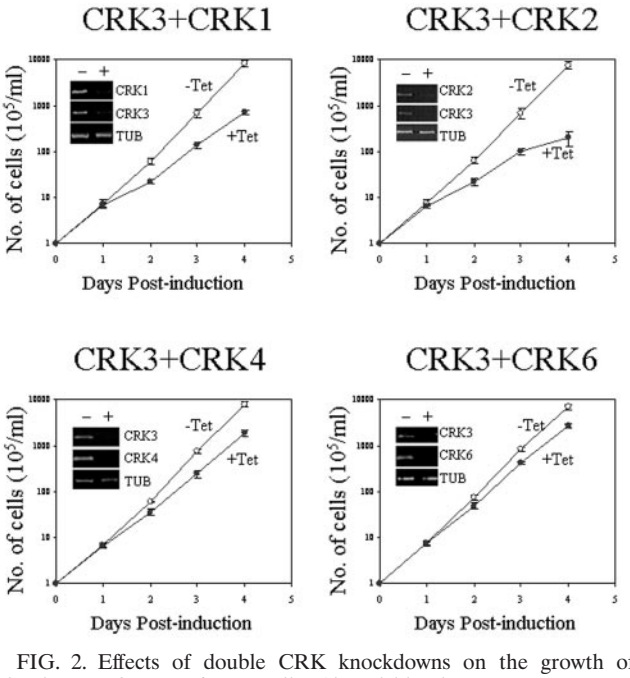

FIG. 2. Effects of double CRK knockdowns on the growth of bloodstream-form *T. brucei* cells. Cloned bloodstream trypanosome cells harboring the double CRK RNAi plasmid constructs were each incubated at 37°C in culture medium containing 1.0-μg/ml tetracycline (+Tet) at 37°C. Cell growth was monitored daily, and the cell numbers plotted in a logarithmic scale. The insets show the intracellular mRNA levels in the cells after a 3-day RNAi induction monitored by semiquantitative RT-PCR. Quantitation of α-tubulin mRNA (*TUB*) was included as a sampling control.

pair of DNA fragments was also examined in the Trypanosome Genome Database, and there was no significant sequence identity with other genome sequences. It is thus highly unlikely that, by using these DNA constructs in RNAi experiments, expression of another unidentified gene could be inadvertently knocked down.

The effects of RNAi on individual *CRK* gene expressions were examined by semiquantitative RT-PCR analysis. The results (shown in the insets of Fig. 1 and 2) indicate that, after initiating the RNAi for 3 days, levels of the two *CRK* mRNAs, aimed at by the particular RNAi design, both diminished significantly in each case. The knockdown of gene expression was highly specific, as levels of the other three *CRK* mRNAs that were not included in the original knockdown design always remain unchanged (data not shown). There is thus little doubt that each RNAi experiment presented in Fig. 1 and 2 led to knockdown of only the two specific *CRK* mRNAs originally intended (26).

The effects from simultaneous depletion of *CRK3* mRNA and another *CRK* mRNA on the growth of trypanosome cells were monitored by a daily counting of the cells during a 9-day incubation of the procyclic form and a 4-day incubation of the bloodstream form (Fig. 1 and 2). The results indicate that in the procyclic form, a knockdown of *CRK3* + *CRK2* led to a near total growth arrest, with an estimated growth of only 0.2% of that of the uninduced control. For the rest of the knockdown experiments, the growths of *CRK3* + *CRK1*-, *CRK3* + *CRK4*-, and *CRK3* + *CRK6*-deficient cells were reduced to 1%, 14%, and 4% of the uninduced controls, respectively (Fig. 1). When these results are compared with the 9% growth of the cells with only *CRK3* knocked down (26), one could conclude that CRK1, CRK2, and CRK3 may each play an important role in regulating cell growth whereas CRK4 and CRK6 may play either a minor role or no role at all.

In the bloodstream form, the growths of *CRK3* + *CRK2*-, *CRK3* + *CRK1*-, *CRK3* + *CRK4*-, and *CRK3*+*CRK6*-deficient cells were reduced to 2%, 6%, 16%, and 24% of the uninduced controls, respectively (Fig. 2). When these were compared with the 31% growth of cells with only CRK3 knocked down (26), a similar conclusion could be reached that CRK1, CRK2, and CRK3 each plays a role in cell growth whereas CRK4 and CRK6 may not.

Effects of double CRK depletions on cell cycle progression of *T. brucei*. For the procyclic form, FACS analysis of the cell population by their DNA content indicated that after the expression of *CRK3*+ *CRK2* was knocked down for 5 days, cells in the G_1 phase were reduced from approximately 43% to 19% of the population. The G_2/M-phase cells were enhanced from 17% to 40%, whereas the S-phase cells showed no apparent change (Fig. 3). Among the CRK3 + CRK4- and CRK3 + CRK6-depleted cells, there were also 24% and 23% decreases of G_1-phase cells accompanied by 28% and 21% increases of G_2/M-phase cells but only slight changes in the S-phase population (Fig. 3). These data are essentially identical to those from the cells with only a CRK3 deficiency, which had a de-

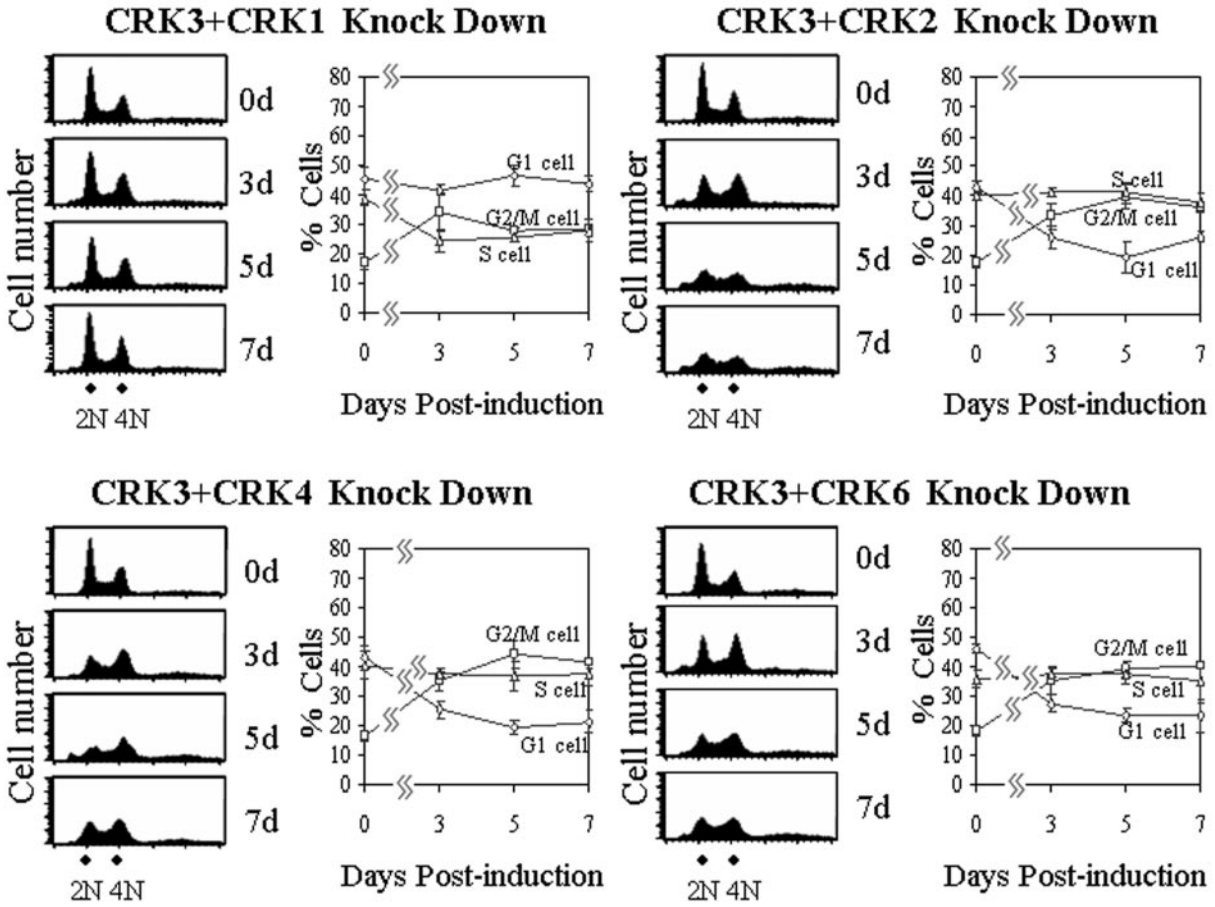

FIG. 3. FACS analysis of double CRK-deficient procyclic-form *T. brucei* cells. Time samples of RNAi-induced procyclic-form *T. brucei* cells were stained with PI and subjected to FACS analysis for DNA content. The histograms from FACScan are presented on the left-hand side of each panel. The percentages of cells in G_1, S, and G_2/M phases were determined with ModFitLT software and plotted on the right-hand side of each panel.

crease of the G_1 population from 45 to 15%, an increase of G_2/M-phase cells from 20 to 50%, and a virtually unchanged S-phase population (26). This lack of difference suggests that CRK2, CRK4, and CRK6 are unlikely to play a significant role in controlling G_2/M checkpoint passage in the procyclic form of *T. brucei*. When CRK1 and CRK3 were knocked down together, the population of G_2/M-phase cells was increased only from 17% to 28%. The percentage of G_1-phase cells remained unchanged, whereas S-phase cells were decreased slightly from approximately 39% to 26% of the population (Fig. 3). In comparison with the outcomes from the three previous double-knockdown experiments, the virtual stagnation of progression across both G_1/S and G_2/M checkpoints indicates that while CRK3 alone may control the G_2/M checkpoint, CRK1 regulates G_1/S passage, as previously indicated in the single CRK1 knockdown experiment (26).

Similar results from FACS analysis were also observed in the bloodstream form. After knocking down the expression of CRK3 + CRK2, CRK3 + CRK4, and CRK3 + CRK6 for 3 days, there were 18%, 29%, and 33% reductions of G_1-phase cells accompanied by 23%, 28%, and 28% increases of G_2/M-phase cells and only slight changes in the S-phase population, respectively (Fig. 4). These data bear significant similarity to those from bloodstream-form *T brucei* cells with only a single CRK3 knockdown, where a 20% enhancement in the G_2/M-phase, a 20% decrease in the G_1-phase, and no significant change in the S-phase populations were observed (26). CRK2, CRK4, and CRK6 thus do not perform an appreciable function in the G_2/M transition of bloodstream-form cells either. When a double knockdown of CRK1 and CRK3 was performed in the bloodstream form, there was an ~8% decrease in G_1-phase, an ~6% increase in G_2/M-phase, and virtually no change in S-phase populations (Fig. 4), confirming an important role of CRK1 in the G_1/S transition in the bloodstream form as well.

In summarizing all the data obtained thus far, CRK3 is without a doubt the only protein kinase regulating G_2/M transition, whereas CRK1 plays an essential role in controlling G_1/S passage in both procyclic and bloodstream forms of *T. brucei*.

Distinct morphologies of procyclic and bloodstream forms with the same double CRK deficiencies. The propidium iodide (PI)-stained double CRK-depleted trypanosome cells were examined under a fluorescence microscope for cells with one nucleus and one kinetoplast (1N1K), one nucleus and two kinetoplasts (1N2K), two nuclei and two kinetoplasts (2N2K),

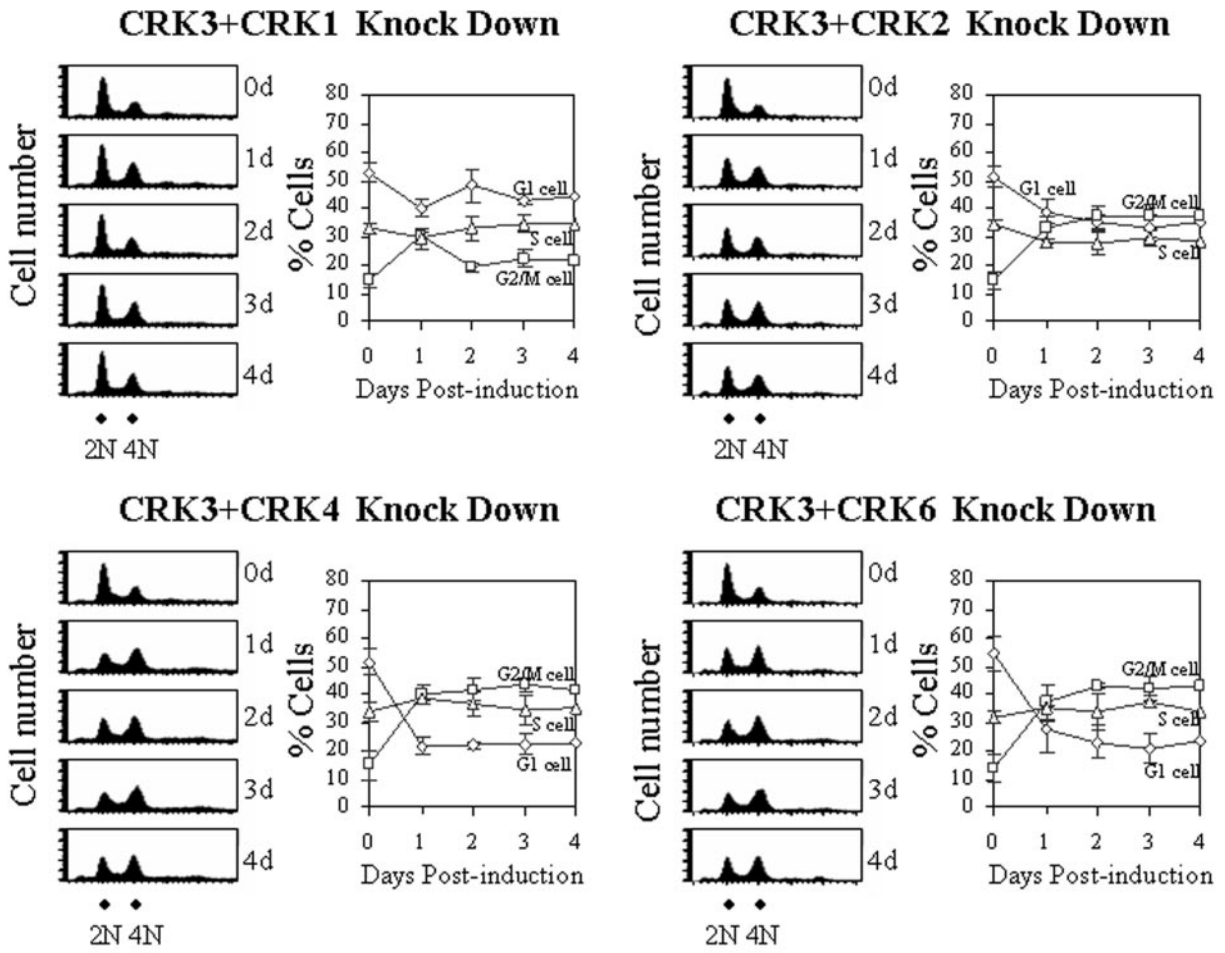

FIG. 4. FACS analysis of double CRK-deficient bloodstream-form *T. brucei* cells. Time samples of RNAi-induced bloodstream-form *T. brucei* cells were stained with PI and subjected to FACS analysis for DNA content. The histograms from FACScan are presented on the left-hand side of each panel. The percentages of cells in G_1, S, and G_2/M phases were determined with ModFitLT software and plotted on the right-hand side of each panel.

no nucleus and one kinetoplast (0N1K, the zoid), and a multiple nuclear aggregate and multiple kinetoplasts (XNXK). An enrichment of cells with somewhat enlarged and occasionally irregularly shaped nuclei was commonly observed among these transfectants. They could be the consequence of a first-round mitotic arrest and are labeled N* when the morphology of such individual cells was compared with that of the control (Fig. 5B).

In the procyclic form of *T. brucei*, CRK3 + CRK2 deficiency resulted in a decrease of the 1N1K population from 76 to 59%, an increase of 1N2K from 13 to 16%, a decrease of 2N2K from 8 to 2%, and an increase of the zoid population from 0 to 20% (Fig. 5A). These are anticipated changes from a mitotic arrest of procyclic forms similar to that resulting from knocking down CRK3 alone (26). *CRK3*+ *CRK4* and *CRK3*+ *CRK6* double knockdowns resulted in a similar extent of morphological changes among the cells (data not shown), suggesting once again that CRK2, CRK4, and CRK6 have little function in regulating G_2/M passage. The CRK3 + CRK1-deficient cells had a more limited morphological shift when compared to the control. There was only a 10% decrease of 1N1K cells and an 11% increase in the zoid population (data not shown), suggesting a near freezing of cell cycle progression at both G_1/S and G_2/M checkpoints and a regulatory role of CRK1 in G_1/S transition.

The emergence of stumpy zoids up to 20% of the population and a considerable percentage of 1N1K cells diminished into the 1N*1K form indicate that kinetoplast segregation, cytokinesis, and cell division were not affected by mitotic arrest (Fig. 5B). The cell cycle is apparently still driven by the kinetoplast cycle and progresses continuously in mitotically arrested procyclic-form *T. brucei*.

Among the CRK3 + CRK2-deficient procyclic-form cells, an apparently normal cellular morphology was maintained (Fig. 5B). They differ from the CRK1 + CRK2-deficient procyclic-form cells arrested in G_1 phase, which possess grossly elongated/branched posterior ends (27). This discrepancy between the two mutants suggests that CRK2 may play a role in regulating morphogenesis of the posterior end of the procyclic form only during the G_1 phase of the cell cycle.

In the bloodstream form of *T. brucei,* CRK3 + CRK2-depleted cells showed, 3 days after induction of RNAi, a decrease

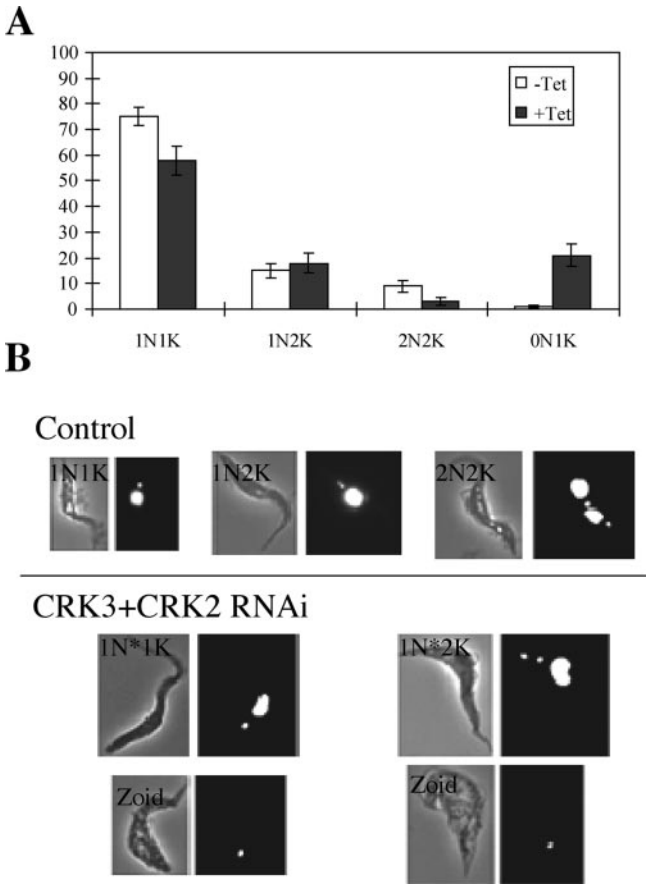

FIG. 5. The morphological phenotype of CRK3 + CRK2-deficient procyclic-form *T. brucei* cells. The procyclic-form *T. brucei* cells 5 days after RNAi induction for knocking down expression of CRK3 + CRK2 were stained with PI and examined under a fluorescence microscope. (A) Quantification of cells with different numbers of nuclei and kinetoplasts. N, nucleus: K, kinetoplast. (B) Upper panel, control 1N1K, 1N2K, and 2N2K cells without RNAi induction. Lower panel, CRK3 + CRK2-knockdown cells showing the 1N*1K, 1N*2K, and 0N1K (zoid) phenotypes.

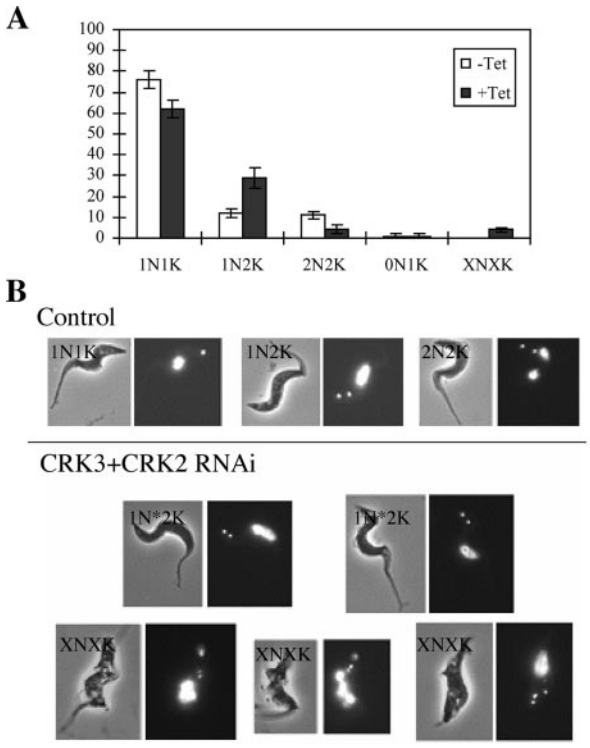

FIG. 6. Morphological phenotype of CRK3 + CRK2-deficient bloodstream-form *T. brucei* cells. The bloodstream-form *T. brucei* cells 3 days after RNAi induction for knocking down expression of CRK3 + CRK2 were stained with PI and examined under a fluorescence microscope. (A) Quantification of cells with different numbers of nuclei and kinetoplasts. N, nucleus: K, kinetoplast. (B) Upper panel, control 1N1K, 1N2K, and 2N2K cells without RNAi induction. Lower panel, the CRK3 + CRK2-knockdown cells showing 1N*2K and XNXK phenotypes.

from 78% to 60% 1N1K cells, a reduction from 8 to 3% 2N2K cells, an enhancement of the 1N2K population from 10 to 30%, and an emergence of 4% XNXK cells (Fig. 6A). Zoids were apparently missing from the population. The diminished population in 1N1K and 2N2K was replaced by a significant increase in 1N2K and XNXK, suggesting in the bloodstream form an unhindered kinetoplast segregation and even multiple nuclear reentries into the G_1 phase during mitotic arrest. But there is apparently no cytokinesis or cell division, which may constitute a major distinction from the procyclic form. The three examples of XNXK cells in Fig. 6B each contains multiple kinetoplasts but only a single aggregate of what appears to be multiple nuclei, suggesting a block of nuclear division. Similar observations were also made from the CRK3 + CRK4 and CRK3 + CRK6 double knockdowns (data not shown) as well as the CRK3 single knockdown (26). In the CRK3 + CRK1-deficient cells, a much less pronounced decrease in the 1N1K population and a less obvious enhancement of 1N2K (data not shown) suggested once again a regulatory role for CRK1 in G_1/S transition.

Further characterizations of the double CRK knockdown cells. The apparent blockade of the mitotically arrested bloodstream-form cells from entering cytokinesis/cell division did not reveal exactly how far the kinetoplast cycle-driven events could proceed before the block. Is the basal body duplicated and new flagellum grown from it to full length prior to the stoppage? If multiple reentries into G_1 and S phases are possible under the arrest, will it be possible to observe multiple basal bodies associated with multiple kinetoplasts and multiple flagella in the XNXK cells? To answer these questions, we stained the cells with YL1/2 (Chemicon), an antibody specific for tyrosinated α-tubulin, and an anti-PFR antibody (ROD1 from Keith Gull of Oxford University) that stains the flagellum of *T. brucei* (35) and examined the stained cells in immunofluorescence assays. YL1/2 is known to stain the newly assembled microtubules and has been useful in identifying the basal body in trypanosomes (12, 32, 33). The YL1/2- and ROD1-stained 1N1K control cells (Fig. 7A) indicate the presence of one basal body that is closely associated with a DAPI-stained kinetoplast. There is also a single flagellum extending out from the basal body. Four CRK3 + CRK2-deficient XNXK cells doubly stained with YL1/2 and ROD1 antibodies (Fig. 7B) demonstrate the presence of multiple basal bodies, each closely associated with a DAPI-stained kinetoplast. Multiple flagella are

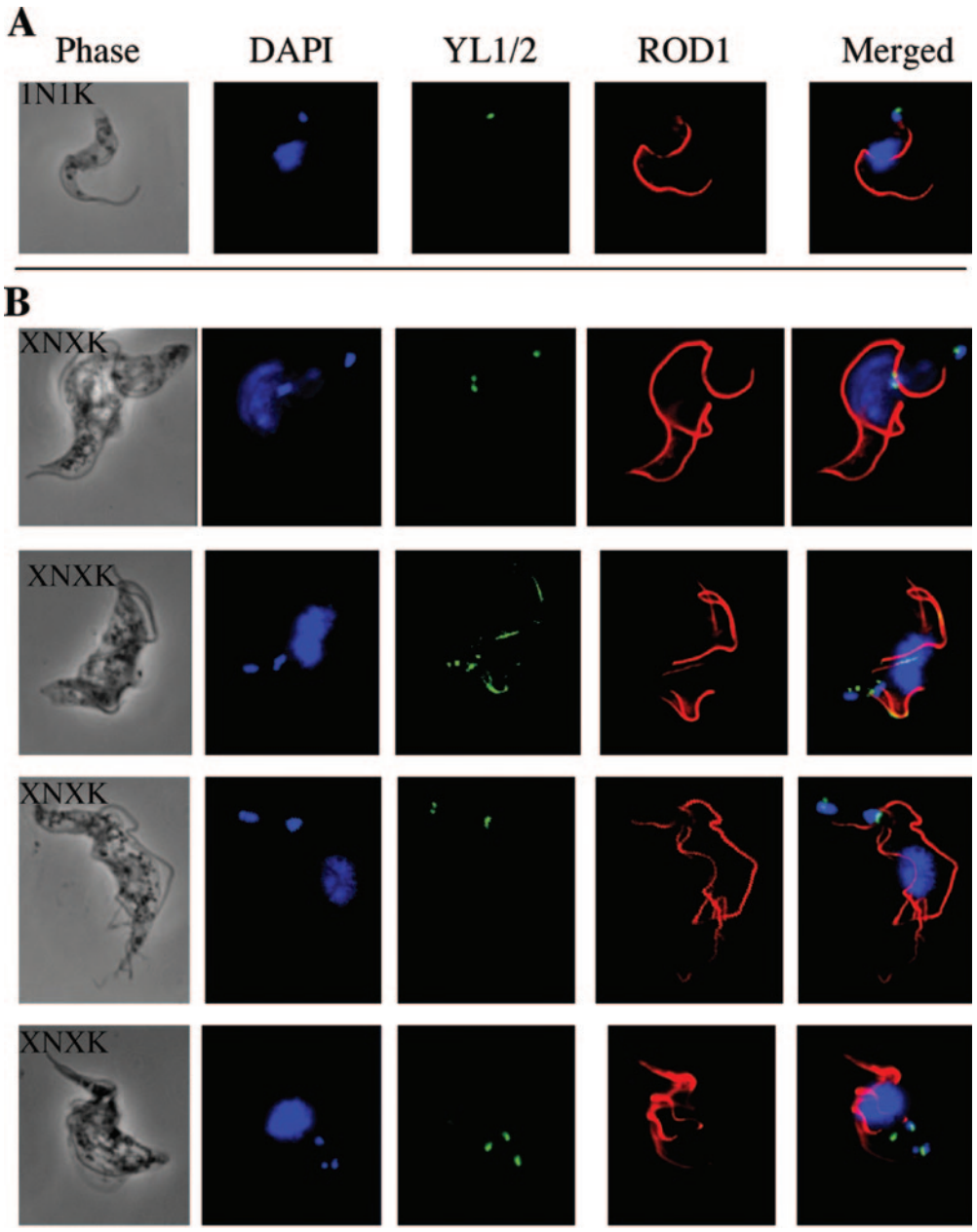

FIG. 7. Double immunofluorescence assay of CRK3 + CRK2-deficient bloodstream-form *T. brucei* cells. The bloodstream-form *T. brucei* cells 3 days after CRK3 + CRK2 RNAi induction were stained with DAPI for DNA, YL1/2 for tyrosinated α-tubulin, and ROD1 for the PFR and examined under a fluorescence microscope. (A) A 1N1K control cell without RNAi induction. (B) CRK3 + CRK2-deficient XNXK cells. ROD1 stained the flagellum, whereas YL1/2 stained the basal body and the newly assembled microtubules.

also found associated with the cells, with each flagellum growing out from a corresponding basal body and extending toward the anterior portion of the cells. There is no indication of flagellum detachment from the cell body, implying completion of all the cellular events up to the point of mitotic exit. There is no indication of cell division from the anterior ends of these cells. The arrest of mitosis has thus apparently blocked all the events beyond G_2. But, reentries into the next G_1 phase have apparently occurred, resulting in the XNXK morphology.

Finally, the CRK1 + CRK2-deficient procyclic forms of *T. brucei* arrested in G_1 phase are known to have their elongated and/or branched posterior ends stained strongly by YL1/2 antibody (Fig. 8C), suggesting that the region is filled with newly synthesized microtubules (27). Since the CRK3 + CRK2-deficient procyclic-form cell does not possess an elongated posterior end (Fig. 5B), it is unclear whether the CRK2 deficiency in this mutant would still lead to excessive microtubule synthesis, but the newly synthesized microtubules may not locate to the posterior end. To clarify this point, four examples of CRK3 + CRK2-deficient cells stained with YL1/2 and ROD1 are presented in Fig. 8B. These samples, including an 1N*1K, an 1N*2K, and two zoids, demonstrate the presence of basal bod-

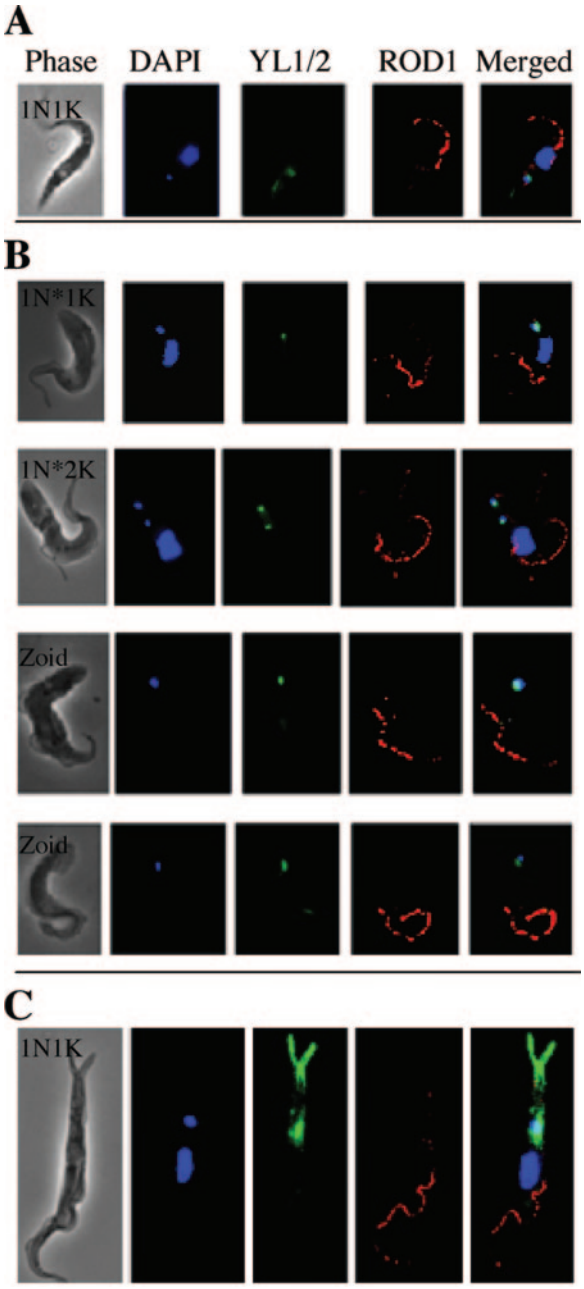

FIG. 8. Double immunofluorescence assay of CRK3 + CRK2-deficient procyclic-form *T. brucei* cells. The procyclic-form *T. brucei* cells 5 days after CRK3 + CRK2 RNAi induction were stained with DAPI for DNA, YL1/2 for tyrosinated α-tubulin, and ROD1 for the PFR and examined under a fluorescence microscope. (A) A 1N1K control cell without RNAi induction. (B) CRK3 + CRK2-deficient 1N*1K and 1N*2K cells and zoids. (C) A CRK1 + CRK2-deficient procyclic-form 1N1K cell with elongated and branched posterior ends. ROD1 stained the flagellum, whereas YL1/2 stained the basal body and the newly assembled microtubules.

ies corresponding to the number and location of kinetoplasts in each cell. There is also only a single flagellum associated with each 1N*1K or zoid cell. There is, however, no indication of newly synthesized microtubules anywhere in the cell, which is in stark contrast to the CRK1 + CRK2-deficient cells with extended posterior ends filled with newly synthesized microtubules (Fig. 8C) (27). This distinction between the two mutants indicates that loss of CRK2 during the G_2/M phase does not lead to uncontrolled microtubule extension toward the posterior end. It occurs only during the G_1 phase of the cell cycle, suggesting a close association between G_1/S transition and posterior morphogenesis in the procyclic form of *T. brucei*.

DISCUSSION

In the present study, we demonstrated that by knocking down the expression of CRK3 plus CRK2, -4, or -6 in both forms of *T. brucei*, the cells were arrested in the G_2/M phase, similar to when only CRK3 was knocked down (26). When CRK3 and CRK1 were depleted simultaneously, cells were trapped at both G_1 and G_2/M phases. These data reinforce the conclusion that CRK1 controls transition across G_1/S and CRK3 regulates the G_2/M checkpoint passage in trypanosomes. CRK2, CRK4, and CRK6 are apparently not involved in cell cycle regulation in this organism.

The CRK1 of *T. brucei* is a 34-kDa protein, sharing about 50% sequence identities with the cdc2 from yeast and CDK2 from humans (18), which are both involved in G_1/S checkpoint regulation. CRK1 has an 84% sequence identity with another cdc2-related protein kinase from *Trypanosoma cruzi*, TzCRK1 (4). TzCRK1 is known to coimmunoprecipitate with mammalian cyclins E, D3, and A and interact with three *T. cruzi* PHO80-like cyclins, TzCYC4, -5, and -6 (4, 5). Our previous observation that an RNAi knockdown of a PHO80 homologue, CycE1/CYC2, from procyclic-form *T. brucei* arrested the cells in G_1 phase (14) and our recent identification of binding between CRK1 and CycE1/CYC2 in yeast two-hybrid assays (S. Gourguechon and C.C. Wang, unpublished results) suggest that these two proteins could be the CDK/cyclin pair controlling the G_1/S checkpoint in both forms of *T. brucei*.

Homologues of CRK3 have also been identified and isolated from *T. cruzi* (TzCRK3) (4), *Leishmania mexicana* (LmmCRK3) (6), and *Leishmania major* (LmajCRK3) (30), sharing over 75% sequence identities. But CRK3 has only around 50% identity to human CDK1. *LmmCRK3* is an essential gene in *L. mexicana* (10) capable of complementing a *Schizosaccharomyces pombe cdc2-33^{ts}* mutant, demonstrating that it can carry out the *cdc2* function in fission yeast (30). Using immunoprecipitation and a yeast two-hybrid screen, CRK3 from *T. brucei* was found associated with a mitotic cyclin homologue, CycB2/CYC6, which was found indispensable for controlling G_2/M passage in both forms of *T. brucei* (9, 28). This pair of proteins is thus the essential CDK/cyclin for initiating passage through the G_2/M checkpoint in *T. brucei* (9, 14, 26).

Our present study has also further established the intriguing distinctions between mitotically arrested procyclic and bloodstream forms of *T. brucei*. While the former can still proceed with cytokinesis and cell division to generate anucleated zoids, the latter is apparently incapable of entering cytokinesis. The nucleus in the procyclic form exhibits the typical appearance of a mitotically arrested N*, whereas the arrested bloodstream form does not prevent nuclear reentry into G_1 for another cycle or the replication of the kintetoplast, as if the cessation of cytokinesis/cell division sends no signal to halt either the nuclear cycle or the kinetoplast cycle. Furthermore, duplication

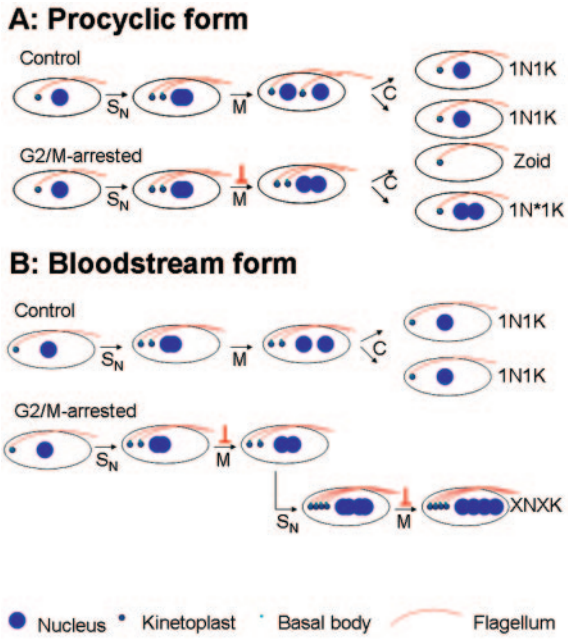

FIG. 9. A model showing distinctive responses to G_2/M arrest by the procyclic and the bloodstream forms of *T. brucei*. S_N, nuclear S phase; M, mitosis; C, cytokinesis. Note the location of kinetoplasts in the midregion of the procyclic form but in the far posterior end of the bloodstream form. Note also in the controls that the two nuclei are partitioned between the two kinetoplasts prior to cytokinesis in the procyclic form. No such partition occurs in the bloodstream form.

of basal bodies and subsequent growth of new flagella from the newly formed basal bodies proceed unabated in the bloodstream form. The newly synthesized flagella have apparently reached their full length and become well separated from one another without initiating cell division from the anterior end (Fig. 7B).

In the trypanosome cell, the daughter flagellum grows out from the basal body near the posterior pole following maturation of the pro-basal body and extends towards the anterior end. It is physically attached to the cell body via the flagellum attachment zone (FAZ), which may provide the structural information required to position the cleavage furrow (23). Trypanosomes with structural defects in the FAZ have problems in cytokinesis (20). As the flagellum defines the positioning of the FAZ, outgrowth of the new flagellum can be viewed as a pivotal event in trypanosome morphogenesis. Recent studies revealed that in procyclic trypanosomes the distal tip of the new flagellum is physically tethered to the site of the old flagellum by a novel structure termed the flagellum connector or FC (17). It was suggested that the physical connection provided by the FC ensures that the new flagellum traces the same helical path along the old flagellum, thus implicating cytotaxis in trypanosome morphogenesis. Despite the apparent importance of the FC in procyclic trypanosomes, conclusive evidence for this structure in the bloodstream form has not yet been forthcoming. This could contribute as a crucial factor in determining the different phenotypes between the two forms. In the procyclic form, the FC imposes a strong force on the starting point of the flagellum and its associated basal bodies located midway between the nucleus and posterior tip of the cells. It eventually triggers or helps cytokinesis following the segregation of kinetoplasts and basal bodies independent of mitosis. However, in the bloodstream form, the lack of this FC structure-derived force may prevent the mitotically arrested cells from passing through cytokinesis/cell division, even though the kinetoplasts and basal bodies have already moved apart and the new flagella have fully grown and separated from each other. This could be the simplest explanation for the distinction of cell cycle regulation between the two forms of the same organism. A model is presented in Fig. 9 to illustrate the distinctive events following a G_2/M arrest in the procyclic and the bloodstream forms of *T. brucei*.

Another unexpected observation made in the present study is that while CRK2 deficiency during G_1 arrest of the procyclic form causes formation of grossly elongated/branched posterior ends filled with newly synthesized microtubules (27), the same CRK2 loss during G_2/M arrest of the same cells does not lead to such a phenotype. The internal cytoskeleton of *T. brucei* is characterized by a subpellicular corset of microtubules with their positive ends all pointed toward the posterior end of the cell (7), suggesting a unified cortical microtubule extension toward this end. During cell division, separation between the two daughter cells begins from the anterior end and progresses toward the posterior end, which provides the final point of connection between the two. A simple hypothesis would be that active cortical microtubule extension toward the posterior ends of two daughter cells should occur in the late phase of cell division. But our experimental evidence indicates that it instead happens during the G_1 phase and is terminated by the action of CRK2 during the G_1/S transition. Thus, when cells are in G_2/M, there is apparently little active cortical microtubule extension, and a knockdown of CRK2 during this phase does not result in uncontrolled microtubule synthesis. More protein kinases have been implicated in mediating cytoskeletal modulations in recent studies. A good example could be the p21-activated kinase family (PAK), which is represented by Shk1 and Ste20 from yeast, XPAK5 from *Xenopus*, and HsPAKs from humans (3, 15). As a first step of looking into whether CRK2 possibly belongs to the PAK family, it will be important to know the time profile of CRK2 expression during the cell cycle as well as the potential effect of overexpressing CRK2 during the G_1 and G_2/M phases of procyclic-form *T. brucei.*

ACKNOWLEDGMENTS

We thank W. Zacheus Cande of UC Berkeley for his valuable and stimulating discussions with us during the progression of this work and his comments and suggestions on the manuscript. We are also grateful to Lee Douglas of UC Berkeley for reading the manuscript and for his constructive suggestions. Gratitude goes also to Keith Gull, Oxford University, for the generous gift of ROD1.

This study was supported by NIH grant AI-21786.

REFERENCES

1. **Bastin, P., K. Ellis, L. Kohl, and K. Gull.** 2000. Flagellum ontogeny in trypanosomes studied via an inherited and regulated RNA interference system. J. Cell Sci. **113:**3321–3328.
2. **Carruthers, V. B., and G. A. Cross.** 1992. High-efficiency clonal growth of bloodstream- and insect-form Trypanosoma brucei on agarose plates. Proc. Natl. Acad. Sci. USA **89:**8818–8821.
3. **Cau, J., S. Faure, M. Comps, C. Delsert, and N. Morin.** 2001. A novel p21-activated kinase binds the actin and microtubule networks and induces microtubule stabilization. J. Cell Biol. **155:**1029–1042.

4. **Gómez, E. B., A. R. Kornblihtt, and M. T. Téllez-Iñón.** 1998. Cloning of a cdc2-related protein kinase from Trypanosoma cruzi that interacts with mammalian cyclins. Mol. Biochem. Parasitol. **91:**337–351.
5. **Gómez, E. B., M. I. Santori, S. Laria, J. C. Engel, J. Swindle, H. Eisen, P. Szankasi, and M. T. Téllez-Iñón.** 2001. Characterization of the Trypanosoma cruzi Cdc2p-related protein kinase 1 and identification of three novel associating cyclins. Mol. Biochem. Parasitol. **113:**97–108.
6. **Grant, K. M., P. Hassan, J. S. Anderson, and J. C. Mottram.** 1998. The crk3 gene of Leishmania mexicana encodes a stage-regulated cdc2-related histone H1 kinase that associates with p12. J. Biol. Chem. **273:**10153–10159.
7. **Gull, K.** 1999. The cytoskeleton of trypanosomatid parasites. Annu. Rev. Microbiol. **53:**629–655.
8. **Hammarton, T. C., J. C. Mottram, and C. D. Doerig.** 2003. The cell cycle of parasitic protozoa: potential for chemotherapeutic exploitation. Prog. Cell Cycle Res. **5:**91–101.
9. **Hammarton, T. C., J. Clark, F. Douglas, M. Boshart, and J. C. Mottram.** 2003. Stage-specific differences in cell cycle control in Trypanosoma brucei revealed by RNA interference of a mitotic cyclin. J. Biol. Chem. **278:**22877–22886.
10. **Hassan, P., D. Fergusson, K. M. Grant, and J. C. Mottram.** 2001. The CRK3 protein kinase is essential for cell cycle progression of Leishmania mexicana. Mol. Biochem. Parasitol. **113:**189–198.
11. **Hirumi, H., and K. Hirumi.** 1989. Continuous cultivation of Trypanosoma brucei blood stream forms in a medium containing a low concentration of serum protein without feeder cell layers. J. Parasitol. **75:**985–989.
12. **Kilmartin, J. V., B. Wright, and C. Milstein.** 1982. Rat monoclonal antitubulin antibodies derived by using a new nonsecreting rat cell line. J. Cell Biol. **93:**576–582.
13. **Klingbeil, M. M., S. A. Motyka, and P. T. Englund.** 2002. Multiple mitochondrial DNA polymerases in Trypanosoma brucei. Mol. Cell **10:**175–186.
14. **Li, Z., and C. C. Wang.** 2003. A PHO80-like cyclin and a B-type cyclin control the cell cycle of the procyclic form of Trypanosoma brucei. J. Biol. Chem. **278:**20652–20658.
15. **Marcus, S., A. Polverino, E. Chang, D. Robbins, M. H. Cobb, and M. H. Wigler.** 1995. Shk1, a homolog of the Saccharomyces cerevisiae Ste20 and mammalian p65PAK protein kinases, is a component of a Ras/Cdc42 signaling module in the fission yeast Schizosaccharomyces pombe. Proc. Natl. Acad. Sci. USA **92:**6180–6184.
16. **Matthews, K. R., T. Sherwin, and K. Gull.** 1995. Mitochondrial genome repositioning during the differentiation of the African trypanosome between life cycle forms is microtubule mediated. J. Cell Sci. **108:**2231–2239.
17. **Moreira-Leite, F. F., T. Sherwin, L. Kohl, and K. Gull.** 2001. A trypanosome structure involved in transmitting cytoplasmic information during cell division. Science **294:**610–612.
18. **Morgan, D. O.** 1997. Cyclin-dependent kinases: engines, clocks, and microprocessors. Annu. Rev. Cell Dev. Biol. **13:**261–291.
19. **Mottram, J. C., and G. Smith.** 1995. A family of trypanosome cdc2-related protein kinases. Gene **162:**147–152.

19a. **Mutomba, M. C., W.-Y. To, W. C. Hyun, and C. C. Wang.** 1997. Inhibition of proteasome activity blocks cell cycle progression at specific phase boundaries in African trypanosomes. Mol. Biochem. Parasitol. **90:**491–504.

20. **Ngo, H., C. Tschudi, K. Gull, and E. Ullu.** 1998. Double-stranded RNA induces mRNA degradation in Trypanosoma brucei. Proc. Natl. Acad. Sci. USA **95:**14687–14692.
21. **Ploubidou, A., D. R. Robinson, R. C. Docherty, E. O. Ogbadoyi, and K. Gull.** 1999. Evidence for novel cell cycle checkpoint in trypanosomes: kinetoplast segregation and cytokinesis in the absence of mitosis. J. Cell Sci. **112:**4641–4650.
22. **Robinson, D. R., and K. Gull.** 1991. Basal body movements as a mechanism for mitochondrial genome segregation in the trypanosome cell cycle. Nature **352:**731–733.
23. **Robinson, D. R., T. Sherwin, A. Ploubidou, E. H. Byard, and K. Gull.** 1995. Microtubule polarity and dynamics in the control of organelle positioning, segregation, and cytokinesis in the trypanosome cell cycle. J. Cell Biol. **128:**1163–1172.
24. **Sherwin, T., and K. Gull.** 1989. The cell division cycle of Trypanosoma brucei brucei: timing of event markers and cytoskeletal modulations. Philos. Trans. R. Soc. Lond. B Biol. Sci. **323:**573–588.
25. **Timms, M. W., F. J. van Deursen, E. F. Hendriks, and K. R. Matthews.** 2002. Mitochondrial development during life cycle differentiation of African trypanosomes: evidence for a kinetoplast-dependent differentiation control point. Mol. Biol. Cell **13:**3747–3759.
26. **Tu, X. M., and C. C. Wang.** 2004. The involvement of two cdc2-related kinases (CRKs) in Trypanosoma brucei cell-cycle regulation and the distinctive stage-specific phenotypes caused by CRK3 depletion. J. Biol. Chem. **279:**20519–20528.
27. **Tu, X. M., and C. C. Wang.** 2005. Coupling of posterior cytoskeletal morphogenesis to the G1/S Transition in the Trypanosoma brucei cell cycle. Mol. Biol. Cell **16:**97–105.
28. **Van Hellemond, J. J., P. Neuville, R. T. Schwarz, K. R. Matthews, and J. C. Mottram.** 2000. Isolation of Trypanosoma brucei CYC2 and CYC3 cyclin genes by rescue of a yeast G(1) cyclin mutant. Functional characterization of CYC2. J. Biol. Chem. **275:**8315–8323.
29. **Vickerman, K.** 1985. Developmental cycles and biology of pathogenic trypanosomes. Br. Med. Bull. **41:**105–114.
30. **Wang, Y., K. Dimitrov, L. K. Garrity, S. Sazer, and S. M. Beverley.** 1998. Stage-specific activity of the Leishmania major CRK3 kinase and functional rescue of a Schizosaccharomyces pombe cdc2 mutant. Mol. Biochem. Parasitol. **96:**139–150.
31. **Wang, Z., J. C. Morris, M. E. Drew, and P. T. Englund.** 2000. Inhibition of Trypanosoma brucei gene expression by RNA interference using an integratable vector with opposing T7 promoters. J. Biol. Chem. **275:**40174–40179.
32. **Wehland, J., M. C. Willingham, and I. V. Sandoval.** 1983. A rat monoclonal antibody reacting specifically with the tyrosylated form of alpha-tubulin. I. Biochemical characterization, effects on microtubule polymerization in vitro, and microtubule polymerization and organization *in vivo.* J. Cell Biol. **97:**1467–1475.
33. **Wehland, J., H. C. Schroder, and K. Weber.** 1984. Amino acid sequence requirements in the epitope recognized by the alpha-tubulin-specific rat monoclonal antibody YL1/2. EMBO J. **3:**1295–1300.
34. **Wirtz, E., S. Leal, C. Ochatt, and G. A. Cross.** 1999. A tightly regulated inducible expression system for conditional gene knock-outs and dominant-negative genetics in Trypanosoma brucei. Mol. Biochem. Parasitol. **99:**89–101.
35. **Woods, A., T. Sherwin, R. Sasse, T. H. MacRae, A. J. Baines, and K. Gull.** 1989. Definition of individual components within the cytoskeleton of Trypanosoma brucei by a library of monoclonal antibodies. J. Cell Sci. **93:**491–500.
36. **Woodward, R., and K. Gull.** 1990. Timing of nuclear and kinetoplast DNA replication and early morphological events in the cell cycle of *Trypanosoma brucei.* J. Cell Sci. **95:**49–57.